Clickable Macroinitiator Strategy to Build Amphiphilic Polymer Brushes on Carbon Nanotubes

Yu Zhang,[†] Hongkun He,[†] and Chao Gao*[,†,‡]

College of Chemistry and Chemical Engineering, Shanghai Jiao Tong University, 800 Dongchuan Road, Shanghai 200240, P. R. China, and Department of Polymer Science and Engineering, Zhejiang University, and Key Laboratory of Macromolecular Synthesis and Functionalization, Ministry of Education, 38 Zheda Road, Hangzhou 310027, P. R. China

Received July 27, 2008; Revised Manuscript Received October 22, 2008

ABSTRACT: A novel and versatile Gemini-grafting strategy to modify surfaces/substrates is presented by a combination of conventional "grafting to" and "grafting from" strategies. As a typical example, carbon nanotubes (CNTs) were functionalized with amphiphilic/Janus polymer brushes by uniting click chemistry with a macroinitiator approach. A clickable macroinitiator, poly(3-azido-2-(2-bromo-2-methylpropanoyloxy)propyl methacrylate) (polyBrAzPMA), with alkyl bromo groups for initiating atom transfer radical polymerization (ATRP) and azido groups for the click reaction was first synthesized by postmodification of poly(glycidyl methacrylate) with sodium azide, followed by 2-bromoisobutyryl bromide. The clickable macroinitiator was clicked onto alkyne-containing multiwalled/single-walled CNTs via the Cu(I)-catalyzed click reaction of Huisgen 1,3-dipolar cycloaddition between azides and alkynes, resulting in a CNT-based clickable macroinitiator. Poly(*n*-butyl methacrylate), polystyrene, and poly(ethylene glycol) were subsequently grown on CNTs via ATRP grafting from and click grafting to approaches, affording CNT-supported amphiphilic polymer brushes. The functionalized CNTs were characterized by thermal gravimetric analysis (TGA), FTIR, Raman spectroscopy, X-ray photoelectron spectroscopy (XPS), scanning electron microscopy (SEM), and transmission electron microscopy (TEM) measurements. All of the results demonstrated that it is feasible and facile to grow various multifunctional polymer brushes on CNTs by the clickable macroinitiator strategy, and the grafted polymer content can be well controlled. This versatile strategy can be readily extended to prepare other Janus/bifunctional polymer brushes, opening an avenue for building complex polymer architectures and tailoring surface properties.

Introduction

Modification of surfaces is of extreme importance, especially for the construction of desirable structures, the gaining of tailor-made properties, and the application of them in expected areas, because the performance of a material is always dependent on its surface property. Until now, two main strategies, "grafting to" and "grafting from", have been presented and widely used to modify a solid surface with polymers, giving rise to so-called polymer brushes.

The "grafting to" strategy is to graft available polymers that normally possess terminal functional groups onto a surface.[1−3]Accordingly, it has several significant advantages. First, the molecular parameters of the used polymers such as chemical structure, molecular weight, and polydispersity index (PDI) can be determined and accurately known. Second, some macromolecules with special chemical structures and functionalities (e.g., dendrons, dendrimers, block copolymers, etc.) can be immobilized on surfaces. Third, the unreacted polymers may be recycled by separation from reaction system via centrifugation or precipitation. Nevertheless, the poor controllability of grafting quantity and the relatively low grafting density attributed to the interferences of the pregrafted polymer chains imply its disadvantages.[4]

The "grafting from" strategy involves growth of polymer chains from a surface by means of surface-initiated polymerization (SIP) of monomers and has merits of good controllability for the grafted polymer content and structure, high and even grafting efficiency, and a wide monomer availability ranging from vinyl to cyclic molecules.[5−8] Recently, Armes et al. reported a new macroinitiator "grafting from" approach to modify silica particles.[9] The positive macroinitiator containing both amino and alkyl bromo groups was physically adsorbed on the negative silica surface via electrostatic force, followed by in situ atom transfer radical polymerization (ATRP) initiated with the bromo groups, which afforded spherical silica polymer brushes. Edmondson et al. reported a new layer-by-layer approach for assembling oppositely charged polyelectrolytic macroinitiators on planar silica substrates to enhance the initiator density for ATRP reaction.[10]

Obviously, it is quite difficult to graft different polymers on the same surface evenly by either "grafting to" or "grafting from" strategies. Nonetheless, it is exceedingly important to fulfill such a dream, especially for the design, tailoring, and fabrication of multifunctional surfaces and materials. Hence, we present a novel strategy for modifying surfaces with multiple kinds of polymers by a combination of "grafting to" and "grafting from" strategies, as depicted in Figure 1. A multifunctional macroinitiator containing both initiating sites for living/controlled polymerization and other reactive groups (e.g., hydroxyl, amino, and carboxyl groups) for condensation is first coated on a surface covalently, generating a multifunctional surface with residual reactive groups of condensation and initiating points. Subsequently, different polymer chains are linked on the multifunctional surface via "grafting to" and "grafting from" manners in one-step/pot or separated steps. The proposed third strategy shows the following characteristics: (1) different polymers can be grafted on a surface evenly and controllably, (2) a versatile surface with multifunctions (e.g., pH and thermal responsive, solvent-recognizable, and other smart surface) can be accessed facilely, and (3) all reactions in the toolbox of organic coupling and polymerization can be employed in modifying a surface. Thus, we coin it as the Gemini-grafting strategy.

* To whom correspondence should be addressed. E-mail: chaogao@zju.edu.cn.
[†] Shanghai Jiao Tong University.
[‡] Zhejiang University.

10.1021/ma801696z CCC: $40.75
Published on Web 11/21/2008

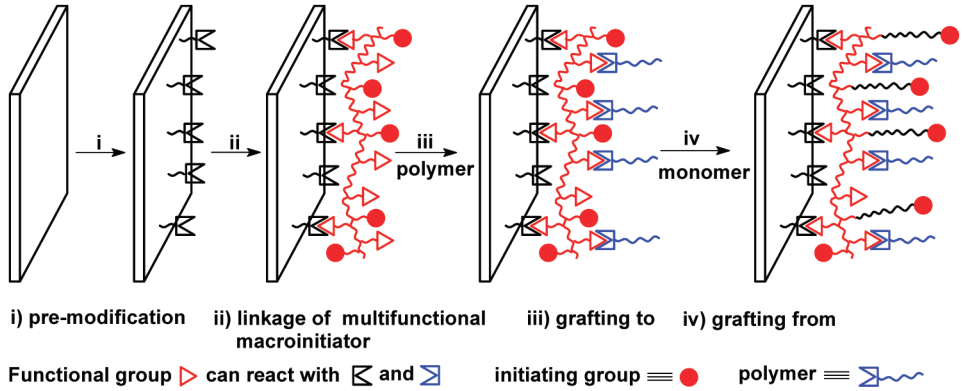

Figure 1. Schematic description of the presented Gemini-grafting strategy to functionalize a surface.

Herein, as a typical example, we adopt ATRP[11−15] and click chemistry[16−21] as polymerization and coupling tools, respectively, to functionalize the cylindrical surface of carbon nanotubes (CNTs) to demonstrate how the Gemini-grafting strategy works because both ATRP and click chemistry of Huisgen 1,3-dipolar cycloaddition between azides and alkynes are powerful techniques that are widely used for the modification of surfaces. Therefore, a clickable macroinitiator possessing azido and bromo groups at each unit is designed and synthesized to click alkyne-contained CNTs, which forms a CNT-based clickable macroinitiator because only a small part of azido groups in the polymer sides are consumed during such a heterogeneous reaction. The bromo and residual azido groups are then used to initiate ATRP and to click alkyne-terminated polymers, respectively, affording amphiphilic/Janus polymer brush-enveloped CNTs. Therefore, we can also call the specific strategy a clickable macroinitiator. There is no doubt that the same protocol as that in the case of CNTs can be easily extended to modify other topological (e.g., linear, spherical, and flat) surfaces.

Experimental Section

Materials. CuBr (Aldrich, 99.999%) was purified according to the published procedures.[22] *N*,*N*,*N*′,*N*″,*N*″-pentmethyldiethylenetriamine (PMDETA, 98%), *N*-hydroxysuccinimide (NHS, 98%), *N*-(3-dimethylaminopropyl)-*N*′-ethylcarbodiimide hydrochloride (EDC·HCl, 99%), *N*,*N*-(dimethylamino)pyridine (DMAP, 98%), ethyl 2-bromoisobutyrate (EBiB, 99%), 2-bromoisobutyryl bromide (98%), 1,3-dicyclohexylcarbodiimide (DCC, 98%), succinic anhydride (98%), and propargyl alcohol (99%) were obtained from Alfa Aesar and were used as received. Triethylamine (TEA), dichloromethane, and styrene (St, Alfa Aesar, 98%) were dried with CaH_2 and distilled under reduced pressure before use. Poly(ethylene glycol) monomethyl ether (PEG-OH, M_n = 1900) was purchased from Aldrich and used as received. We purified glycidyl methacrylate (GMA, 99%, Alfa Aesar) and *n*-butyl methacrylate (nBMA, 99%, Alfa Aesar) by passing the monomers through a column filled with basic alumina to remove the inhibitor. Tetrahydrofuran (THF), methanol, diphenyl ether, dichloromethane (CH_2Cl_2), *N*,*N*-dimethylacetamide (DMF), 1-methyl-2-pyrrolidinone (NMP), thionyl chloride ($SOCl_2$), sodium bicarbonate ($NaHCO_3$), and other organic reagents or solvents were obtained from Shanghai Reagents and were used as received. The multiwalled carbon nanotubes (MWNTs) were purchased from Tsinghua-Nafine Nano-Powder Commercialization Engineering Center in Beijing (purity: >95%, diameters: 10−30 nm, length: >2 μm). The single-walled carbon nanotubes (SWNTs) were purchased from Shenzhen Nanotech Port (purity of CNTs: >90%, purity of SWNTs: >50%). Carboxyl-functionalized MWNTs (MWNT-COOH, ca. 10.9 wt % -COOH groups) were prepared according to previous procedures.[23]

Measurements. Fourier-transform infrared (FTIR) spectra were recorded on a PE Paragon 1000 spectrometer, and all samples were prepared as KBr pellets. Thermal gravimetric analysis (TGA) was measured on a PE TGA-7 instrument with a heating rate of 20 °C/min under nitrogen flow (20 mL·min^{-1}). Raman spectra were collected on a LabRam-1B Raman spectroscope equipped with a 632.8 nm laser source. X-ray photoelectron spectroscopy (XPS) experiments were carried out on an RBD upgraded PHI-5000C ESCA system (Perkin-Elmer) with Mg Kα radiation ($h\nu$ = 1253.6 eV). In general, the X-ray anode was run at 250 W, and the high voltage was kept at 14.0 kV with a detection angle at 54°. ^{1}H NMR spectra were obtained using a Varian Mercury Plus 400 MHz spectrometer. Molecular weights were determined by gel permeation chromatography (GPC) using PE series 200 with an RI-WAT 150CV+ as a detector; BrLi/DMF (0.01 mol/L) was used as the eluent at a flow rate of 1 mL/min, and polystyrene was used as a standard at 70 °C. Scanning electron microscopy (SEM) images were recorded using an LEO 1550VP field-emission microscope, and the samples were loaded onto silicon surfaces. Transmission electron microscopy (TEM) analysis was conducted on a JEOL JEL2010 field-emission electron microscope at 200 kV.

Synthesis of Alkyne-Modified Multiwalled Carbon Nanotubes (MWNT-Alk). Typically, MWNT-COOH (100 mg) was suspended in 2 mL of $SOCl_2$ (32.5 mmol) in a 10 mL round-bottomed flask. This suspension was stirred at 65 °C for 24 h. After the excess $SOCl_2$ was removed under reduced pressure, the flask was cooled in an ice bath. A mixture of propargyl alcohol (1 mL, 16.9 mmol), $CHCl_3$ (2 mL), and anhydrous TEA (1 mL, 7.17 mmol) was added dropwise over a period of 0.5 h under magnetic stirring. The mixture was stirred at 0 °C for 1 h and then at room temperature for 24 h. The solid was separated from the mixture by centrifugation. The collected solid was redispersed in THF (50 mL) and separated by centrifugation. This purification cycle was repeated three times. Then, the collected solid was redispersed in H_2O (50 mL) and separated by centrifugation. This purification cycle was repeated three times. After purification, the resulting solid was dried overnight under vacuum, and an alkyne-modified multiwalled carbon nanotubes (MWNT-Alk) sample (91 mg) was obtained.

Synthesis of 2-Azidoethanol. 2-Azidoethanol was synthesized by the modified Matyjaszewski's method of 3-azidopropanol.[24] Typically, 2-chloroethanol (100 mL, 120.45 g, 1.496 mol), sodium azide (194.49 g, 2 equiv), and water (1000 mL) were added to a 2000 mL flask. The mixture was stirred at 75−78 °C for 96 h. (***Caution!*** *The azide is quite explosively sensitive to friction during feeding and to temperatures of >80 °C.*) After cooling to room temperature, the mixture was extracted with diethyl ether (5 × 100 mL). The organic mixture was dried over magnesium sulfate overnight and concentrated on a rotary evaporator. The obtained residues were distilled under reduced pressure to give a colorless oil in 81% yield. ^{1}H NMR ($CDCl_3$, δ): 3.79 (t, 2H, CH_2O), 3.44 (t, 2H, CH_2N_3), 2.21 (b, 1H, O*H*).

Synthesis of Hydroxyl-Group-Functionalized Single-Walled Carbon Nanotubes (SWNT-OH). Typically, 100 mg of pristine SWNTs was added to 8 mL of NMP in a 25 mL Schlenk flask, and the mixture was dispersed and homogenized by sonicating for 2 h (using ultrasound of 40 kHz frequency). Then, 2-azidoethanol

(10 g, 115 mmol) was added to this Schlenk under N_2, and the mixture was deoxygenated by bubbling with nitrogen for 30 min. The mixture was stirred at 160 °C for 18 h. The resulting products were separated from the mixture by centrifugation. The collected solid was redispersed in acetone (50 mL) and separated by centrifugation. This purification cycle was repeated three times. Then, the collected solid was redispersed in H_2O (50 mL) and separated by centrifugation. This purification cycle was repeated three times. The functionalized SWNTs were dried overnight under vacuum at 60 °C, giving the SWNT-OH sample (91 mg).

Synthesis of 4-Oxo-4-(prop-2-ynyloxy)butanoic Acid. Succinic anhydride (10 g, 0.1 mol), anhydrous TEA (3.03 g, 30 mmol), DMAP (0.37 g, 3.0 mmol), and anhydrous dichloromethane (100 mL) were added to a 200 mL round-bottomed flask. A solution of propargyl alcohol (5.6 g, 0.1 mol) in dichloromethane (10 mL) was added dropwise over a period of 1 h under magnetic stirring. The mixture was stirred at 0 °C for 1 h and then at 40 °C under refluxing for 24 h. Then, the mixture was washed with an aqueous solution of hydrochloric acid (1 M, 3 × 50 mL) and water (1 × 500 mL) and was dried over magnesium sulfate overnight. The solvent was removed on a rotary evaporator, yielding white solids. (14.2 g, yield: 91.1%). ^{1}H NMR ($CDCl_3$, δ): 4.70 (d, 2H, CH_2O), 2.68 (m, 4H, CH_2CH_2), 2.48 (t, 1H, C′CH).

Synthesis of Alkyne-Modified Single-Walled Carbon Nanotubes (SWNT-Alk). In a 100 mL three-mouthed flask with tail gas absorption equipment, 4-oxo-4-(prop-2-ynyloxy)butanoic acid (1.56 g, 10 mmol) was dissolved in anhydrous dichloromethane (10 mL), and the mixture was cooled in an ice water bath. A mixture of $SOCl_2$ (5 mL, 81.3 mmol) and anhydrous dichloromethane (5 mL) was added dropwise over a period of 1 h under magnetic stirring. The mixture was stirred at 0 °C for 1 h and then at room temperature for 24 h. After the solvent and residual $SOCl_2$ were removed on a rotary evaporator, the three-mouthed flask was cooled in an ice bath, and a mixture of 100 mg SWNT-OH, $CHCl_3$ (2 mL), and anhydrous TEA (1 mL) was added dropwise over a period of 0.5 h under magnetic stirring. The mixture was stirred at room temperature for 24 h. The functionalized SWNTs were separated from the mixture by centrifugation. The collected solid was redispersed in THF (50 mL) and separated by centrifugation. This purification cycle was repeated three times. Then, the collected solid was redispersed in H_2O (50 mL) and separated by centrifugation. This purification cycle was repeated three times. After purification, the resulting solid was dried overnight in vacuum, and an alkyne-modified single-walled carbon nanotubes (SWNT-Alk) sample (93 mg) was obtained.

Synthesis of PolyGMA by ATRP.[25] Typically, a mixture containing GMA (7.11 g, 50 mmol), CuBr (35.9 mg, 0.25 mmol), and diphenyl ether (6.6 mL) was deoxygenated by bubbling with nitrogen for at least 30 min. PMDETA (52.6 μL, 0.25 mmol) was introduced under the protection of nitrogen flow. The reaction mixture was stirred for 15 min to allow the formation of the CuBr/PMDETA complex. The reaction mixture was kept at 25 °C, and EBiB (36.7 μL, 0.25 mmol) was added to the mixture under nitrogen flow. The mixture was stirred at 25 °C for 15 min; then, the Schlenk flask was removed from heat and opened to expose the catalyst to air. The mixture was diluted with methylene chloride and passed through a neutral alumina column to remove copper catalyst. The collected eluents were concentrated and precipitated in an excess of *n*-hexane. This purification cycle was repeated twice. The obtained product was dried overnight in a vacuum oven for 24 h to give poly(glycidyl methacrylate) (polyGMA) (5.19 g, M_n = 27 300; M_w/M_n = 1.30).

Synthesis of PolyHAzPMA.[26] PolyGMA (4.26 g, containing about 30 mmol epoxide groups) and DMF (50 mL) were added to a 100 mL round-bottomed flask, and polyGMA was dissolved under magnetic stirring for 0.5 h. Sodium azide (5.85 g, 90 mmol), deionized water (1.62 g, 90 mmol), and sodium bicarbonate (7.56 g, 90 mmol) were added to the flask. The mixture was heated to 50 °C under magnetic stirring for 24 h. The mixture was precipitated in water, and the precipitate was collected and washed with water. The collected precipitate was redissolved in DMF and reprecipitated in water. The obtained product was dried overnight in a vacuum oven for 24 h to give poly(2-hydroxy-3-azidopropyl methacrylate) (polyHAzPMA, 3.97 g, yield: 71.5%, M_n = 36 800; M_w/M_n = 1.36).

Synthesis of Clickable Macroinitiator, PolyBrAzPMA. Clickable macroinitiator polyBrAzPMA with both azido and bromo groups at each unit was synthesized by the acylation reaction of 2-bromoisobutyrate and polyHAzPMA. Typically, a 150 mL round-bottomed flask was charged with polyHAzPMA (3.70 g, containing 20 mmol hydroxyl groups), anhydrous TEA (6.06 g, 60 mmol), and anhydrous DMF (30 mL). The reaction mixture was cooled in an ice water bath. A solution of 2-bromoisobutyryl bromide (3.7 mL, 30 mmol) in DMF (10 mL) was added dropwise over a period of 1 h under magnetic stirring. The mixture was stirred at 0 °C for 1 h and then at room temperature for 24 h. After the insoluble TEA hydrobromide was removed by filtration, the solution was concentrated on a rotary evaporator, followed by precipitation in methanol. The precipitate was collected and redissolved in methylene chloride. The obtained solution was precipitated in an excess of methanol. This purification cycle was repeated twice. The produced polymer was purified by passing through a basic Al_2O_3 column using methylene chloride as eluent. The obtained product was dried overnight in a vacuum oven for 24 h to give poly(3-azido-2-(2-bromo-2-methylpropanoyloxy)propyl methacrylate) (polyBrAzPMA). (3.15 g, yield: 47.2%, M_n = 52 000; M_w/M_n = 1.57).

Synthesis of Monoalkyne-Terminated Poly(ethylene glycol) (PEG-Alk).[26] Typically, PEG-OH (M_n = 1900, 38.0 g, 20 mmol), DMAP (0.27 g, 2.2 mmol), and 4-oxo-4-(prop-2-ynyloxy)butanoic acid (3.43 g, 22 mmol) were added to CH_2Cl_2 (150 mL). The reaction mixture was cooled in an ice water bath, and a solution of DCC (4.53 g, 22 mmol) in CH_2Cl_2 (50 mL) was added dropwise over a period of 1 h under magnetic stirring. The mixture was stirred at 0 °C for 1 h and then at room temperature for 24 h. After the insoluble dicyclohexylurea was removed by filtration, the filtrate was washed with an aqueous solution of hydrochloric acid (1 M, 3 × 200 mL), water (3 × 200 mL), aqueous NaOH (1 M, 3 × 200 mL), and again with water (2 × 200 mL) and was dried over magnesium sulfate overnight. The solvent was removed on a rotary evaporator, and the product was dried overnight in a vacuum oven for 24 h to give PEG-Alk. (33.9 g, yield: 83.2%). ^{1}H NMR ($CDCl_3$, δ): 4.69 (d, 2H, HC′CCH_2O), 4.24 (m, OCH$_2$CH_2OOCCH$_2$CH$_2$-COO, 2H), 3.63 (b, 167H, (OCH_2CH_2O)$_n$), 3.37 (s, CH_3O), 2.67 (s, 4H, OOCCH_2CH_2COO), 2.49 (t, 1H, C′CH).

Grafting Macroinitiator PolyBrAzPMA with Azido Groups on Alkyne-Modified Multiwalled/Single-Walled Carbon Nanotubes by Click Grafting to Approach.[16] MWNT-Alk (70 mg) or SWNT-Alk (70 mg) were suspended in 35 mL of DMF in a 100 mL round-bottomed flask. The suspension was deoxygenated by bubbling with nitrogen for at least 30 min. Macroinitiator polyBrAzPMA with azido groups (polyBrAzPMA, 700 mg), CuBr (60.3 mg, 0.42 mmol), and PMDETA (88.6 μL, 0.42 mmol) were added under the protection of nitrogen flow. The mixture was stirred at room temperature for 24 h. The solid was separated from the mixture by centrifugation. The collected solid was redispersed in DMF (50 mL) and separated by centrifugation. This purification cycle was repeated three times. After purification, the resulting products were dried overnight under vacuum, and a CNT-based clickable macroinitiator MWNT-Br-Az (74.4 mg) or SWNT-Br-Az (73.2 mg) was obtained.

Control Reaction of Multiwalled Carbon Nanotubes and Clickable Macroinitiator under ATRP Conditions. Pristine MWNTs (10 mg) were suspended in 5 mL of DMF in a 10 mL round-bottomed flask. The suspension was deoxygenated by bubbling with nitrogen for at least 30 min. Macroinitiator polyBrAzPMA (100 mg), CuBr (8.6 mg, 0.06 mmol), and PMDETA (12.7 μL, 0.06 mmol) were added under the protection of nitrogen flow. The mixture was stirred at room temperature for 24 h. The solid was separated from the mixture by centrifugation. The collected solid was redispersed in DMF (50 mL) and separated by centrifugation. This purification cycle was repeated three times. After purification, the resulting products were dried overnight under vacuum, and the product was applied to TGA measurement.

Preparation of PnBMA-Grafted MWNTs by in Situ ATRP Initiated with MWNT-Br-Az.[27] Typically, MWNT-Br-Az (50 mg, 0.0193 mmol of Br groups calculated from TGA results), nBMA (0.69 g, 4.82 mmol), and THF (5 mL) were placed in a 10 mL dry flask, which was then sealed with a rubber plug. The mixture was deoxygenated by bubbling with nitrogen for at least 30 min. CuBr (5.5 mg, 0.039 mmol) and PMDETA (8.1 μL, 0.039 mmol) were introduced under the protection of nitrogen flow. The flask was immersed in an oil bath at 30 °C, and its contents were stirred for 24 h. The viscosity increased at the end of the reaction. The mixture was subsequently diluted with THF, and the solid was separated by centrifugation. This purification cycle was repeated three times. The poly(*n*-butyl methacrylate) (PnBMA)-grafted MWNTs with azido groups for subsequent click reaction (MWNT-Az-PnBMA) were obtained after drying overnight under vacuum (50.3 mg).

Grafting Monoalkyne-Terminated Poly(ethylene glycol) (PEG-Alk) on PnBMA-Grafted MWNTs by Click Grafting to Approach.[16] MWNT-Az-PnBMA (25 mg) was suspended in 12.5 mL of DMF in a 50 mL round-bottomed flask. The suspension was deoxygenated by bubbling with nitrogen for at least 30 min. PEG-Alk (250 mg), CuBr (21.5 mg, 0.15 mmol), and PMDETA (31.7 μL, 0.15 mmol) were added under the protection of nitrogen flow. The mixture was stirred at room temperature for 24 h. The solid was separated from the mixture by centrifugation. The collected solid was redispersed in DMF (50 mL) and separated by centrifugation. This purification cycle was repeated three times. After purification, the resulting products were dried overnight under vacuum, and a sample of MWNT-PnBMA-PEG grafted with amphiphilic polymer brushes (23.9 mg) was obtained.

Grafting Monoalkyne-Terminated Poly(ethylene glycol) (PEG-Alk) on SWNT-Br-Az by Click Grafting to Approach.[16] SWNT-Br-Az (50 mg) was suspended in 25 mL of DMF in a 50 mL round-bottomed flask. The suspension was deoxygenated by bubbling with nitrogen for at least 30 min. PEG-Alk (500 mg), CuBr (43.1 mg, 0.30 mmol), and PMDETA (63.3 μL, 0.30 mmol) were added under the protection of nitrogen flow. The mixture was stirred at room temperature for 24 h. The solid was separated from the mixture by centrifugation. The collected solid was redispersed in DMF (50 mL) and separated by centrifugation. This purification cycle was repeated three times. After purification, the resulting products were dried overnight in vacuum, giving PEG-brushes-grafted SWNT-Br-PEG (50.6 mg) with alkyl bromo groups for initiating ATRP.

Grafting Polystyrene Brushes on SWNT-Br-PEG by in Situ ATRP.[28] Typically, SWNT-Br-PEG (25 mg, 0.0072 mmol Br groups calculated from TGA results), styrene (0.395 g, 3.6 mmol), and diphenyl ether (2.5 mL) were placed in a 10 mL dry flask, which was then sealed with a rubber plug. The mixture was deoxygenated by bubbling with nitrogen for at least 30 min. CuBr (2.2 mg, 0.015 mmol) and PMDETA (3.2 μL, 0.015 mmol) were introduced under the protection of nitrogen flow. The flask was immersed in an oil bath at 90 °C, and its contents were stirred for 24 h. The mixture was subsequently diluted with THF, and the solid was separated by centrifugation. After purification, the resulting products were dried overnight in vacuum, giving the sample of SWNT-PEG-PS grafted with amphiphilic polymer brushes (25.9 mg).

Results and Discussion

General Description of the Clickable Macroinitiator Strategy to Functionalize CNTs. Since their discovery in 1991,[29] CNTs have attracted increasing interest as one of the most fascinating nanoobjects because of their unique electronic and mechanical properties and potential applications in the fields of nanofillers, nanodevices, and nanobiotechnology.[30−34] To solubilize CNTs and to make CNT-polymer hybrid materials, a variety of approaches/techniques have been developed to functionalize CNTs, including esterification,[35−37] click coupling,[38] radical coupling,[39−41] anionic coupling,[42,43] γ-ray irradiation,[44] cathodic electrochemical grafting,[45] polycondensation,[46−48] reversible addition−fragmentation chain transfer (RAFT) polymerization,[49−52] nitroxide-mediated radical polymerization (NMRP),[53−55] anionic polymerization,[56−58] ring-opening polymerization (ROP),[59−61] and ATRP.[62−64] These explorations opened a new area of chemistry of CNTs and make the great potential of CNTs realizable in many fields. However, different techniques were rarely used simultaneously to modify the same surface of CNTs. In this article, we create a novel strategy of clickable macroinitiator to functionalize both MWNTs and SWNTs by a combination of grafting to click chemistry and grafting from ATRP approaches.

As for the click chemistry, the Cu(I)-catalyzed azide/alkyne click reaction, a variation of the Huisgen 1,3-dipolar cycloaddition reaction between azides and alkynes, is of particular interest and has been widely used in the design and synthesis of a wide range of functional materials, including functional monomers,[65,66] shell click-cross-linked nanoparticles,[67] dendritic copolymers,[68−72] and functional polymers.[73−79] Hence, our strategy possesses plenty of advantages. First, click chemistry between azides and alkynes has been demonstrated with high efficiency and excellent tolerance to many other functional groups and solvents including water and protonic chemicals,[16,17] and the triazole linkages that result from azides and alkynes are highly stabile to hydrolysis, oxidation, and reduction.[18] Second, the chemical structure, molecular weight, and PDI of presynthesized polymers used for the click reaction are well known. Third, the "grafting from" approach shows good controllability of the grafted polymer content as well as high and even grafting efficiency. Fourth, the macroinitiator not only introduces different functional groups to the surface of CNTs but also plays the role of amplifier of reactive groups. Fifth, Janus/amphiphilic polymer brushes with various functionalities can be readily grown on CNT.

Recently, great efforts have been taken to synthesize Janus particles[80] including Janus micelles,[81−83] Janus cylinders,[84] and Janus discs.[85] Such unique structure can be used in the stabilization of emulsions.[80,86] In this work, our strategy is employed for the first time in constructing Janus/amphiphilic polymer brushes on CNTs. The detailed procedure is shown in Scheme 1. In the first step, the clickable macroinitiator poly-BrAzPMA was clicked to alkyne-contained CNTs, resulting in a CNT-based clickable macroinitiator. Then, hydrophobic poly(nBMA) was grafted from the CNT surface via ATRP. Finally, hydrophilic PEG with a terminal alkyne group was clicked on the azido groups on the poly(nMBA)-grafted CNTs. This route can be called "grafting from first" (route A). Alternatively, "grafting to first" is also a fine method for achieving such an object (route B). It needs hydrophilic PEG to be clicked on the CNT macroinitiator initially, followed by grafting hydrophobic PS from CNTs. (Hereby we choose SWNTs to show the generality of this new strategy.) Interestingly, both click grafting to and ATRP grafting from procedures can be carried out in one pot with the separated addition of reagents or even in one step with the addition of reagents at the same time. This synchronous grafting route is very simple but quite significant. It has been successfully realized in our preliminary explorations and will be published later. We focus on the first two routes in this article.

Preparation of Clickable Macroinitiator. To get well-defined clickable macroinitiators, we prepared polyGMA as a precursor via ATRP,[25] followed by a ring-opening reaction[26] and an acylation reaction to give the corresponding difunctional polymers containing azido groups for the click reaction and alkyl bromo groups for the ATRP reaction, as depicted in Scheme 2. GMA is a kind of functional monomer containing epoxy groups. Hence, we used CuBr/PMDETA as a catalyst and EBiB as an initiator in the polar solvent of diphenyl ether to synthesize polyGMA via ATRP.[25] Good control over molecular weights

Scheme 1. Synthesis of Amphiphilic/Janus Polymer Brushes-Grafted Multiwalled and Single-Walled Carbon Nanotubes (MWNTs and SWNTs) by a Combination of Click Chemistry and Atom Transfer Radical Polymerization (ATRP) Approach[a]

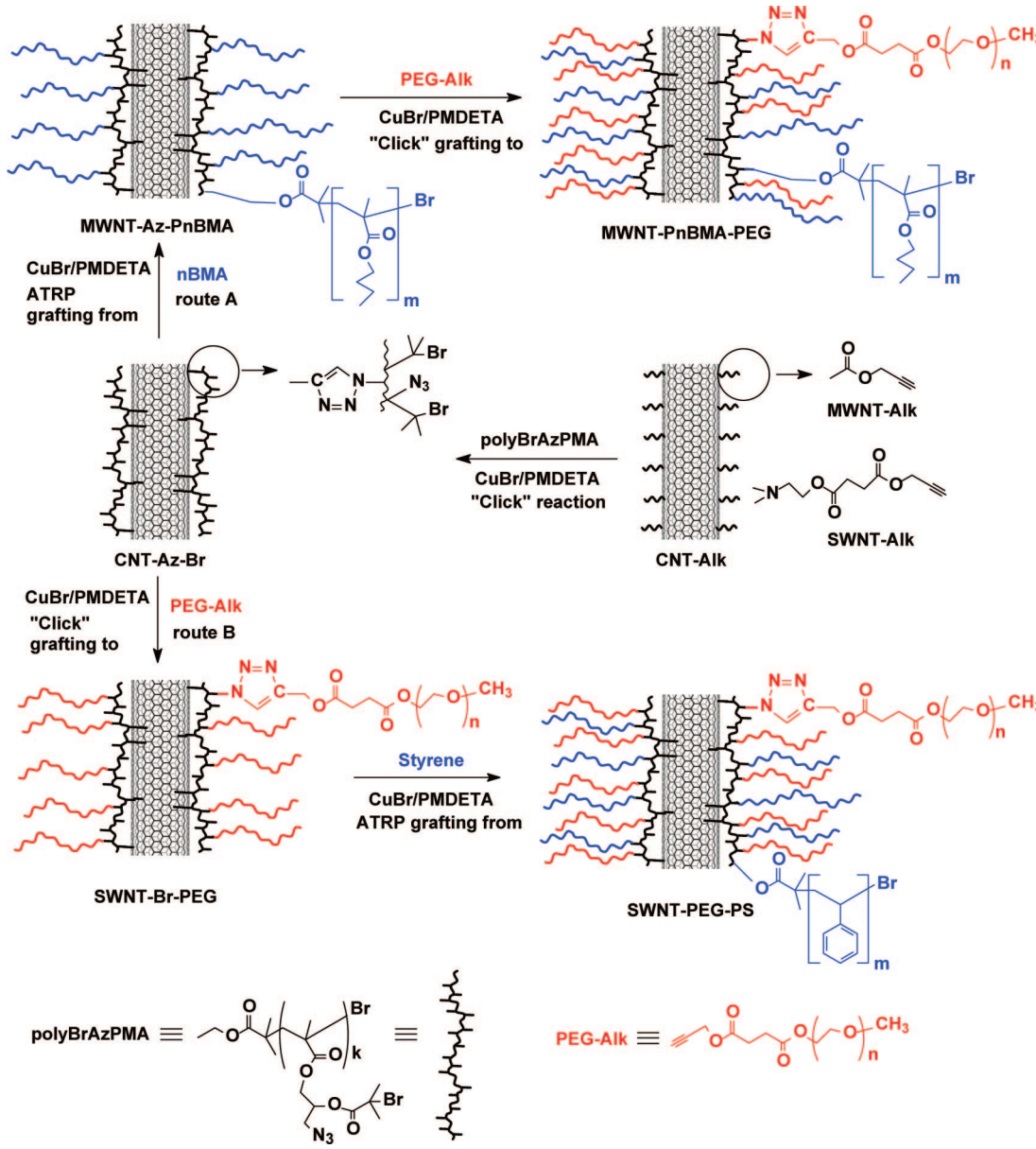

[a] PMDETA: *N,N,N′,N″,N″*-pentmethyldiethylenetriamine, PEG-Alk: monoalkyne-terminated poly(ethylene glycol), CNT-Alk: alkyne-modified carbon nanotubes, CNT-Br-Az: carbon nanotube-based clickable macroinitiator with both kinds of azido and bromo groups (MWNT-Br-Az and SWNT-Br-Az), MWNT-Az-PnBMA: poly(*n*-butyl methacrylate)-grafted MWNTs with azido groups, MWNT-PnBMA-PEG: MWNTs grafted with both poly(*n*-butyl methacrylate) and poly(ethylene glycol) brushes, SWNT-Br-PEG: poly(ethylene glycol)-brushes-grafted single-walled carbon nanotubes with alkyl bromo groups, SWNT-PEG-PS: single-walled carbon nanotubes grafted with both poly(ethylene glycol) and polystyrene brushes.

and low polydispersities (M_n = 27 300; M_w/M_n = 1.30) were observed. In the FTIR spectrum of polyGMA (Figure 2a), the characteristic peaks of carbonyl and epoxy groups are strongly observed at 1730 and 908 cm^{-1}, respectively. All protons of polyGMA are found in the ^1H NMR spectrum (Figure 3a). After modification with sodium azide, the characteristic peak of azido groups at 2106 cm^{-1} was clearly observed in the FTIR spectrum of polyHAzPMA (Figure 2b), and the peak attributed to epoxy groups at 908 cm^{-1} was not observed any more. In the ^1H NMR spectrum of polyHAzPMA (Figure 3b), all of the peaks belonging to the protons from the epoxide ring disappeared, which shows that almost all of the epoxide rings reacted with sodium azide to give new peaks at 5.47 to 5.67 (CH-O*H*) and 3.20 to 3.50 ppm (CH_2N_3). The monomodality in the GPC traces (Figure 4) was observed, which indicated that no coupling or cross-linking happened during the ring-opening reaction. After the esterification reaction between 2-bromoisobutyryl bromide and the hydroxyl groups of polyHAzPMA, clickable macroinitiator polyBrAzPMA was obtained. In the FTIR spectrum of polyBrAzPMA (Figure 2c), the peak of azido groups is still strongly found, and the intensity of carbonyl groups increases. New peaks at ~1.98 ppm ($C(Br)(CH_3)_2$) were clearly observed in the corresponding ^1H NMR spectrum (Figure 3c). All results confirm that the well-defined clickable macroinitiator was successfully synthesized. At least two factors are likely contributed to the phenomenon of the different apparent molecular weights of the polymers with the same backbone mentioned above: (1) the theoretical molecular weights are different from

Scheme 2. Synthesis of Clickable Macroinitiator with Both Kinds of Azido and Bromo Groups[a]

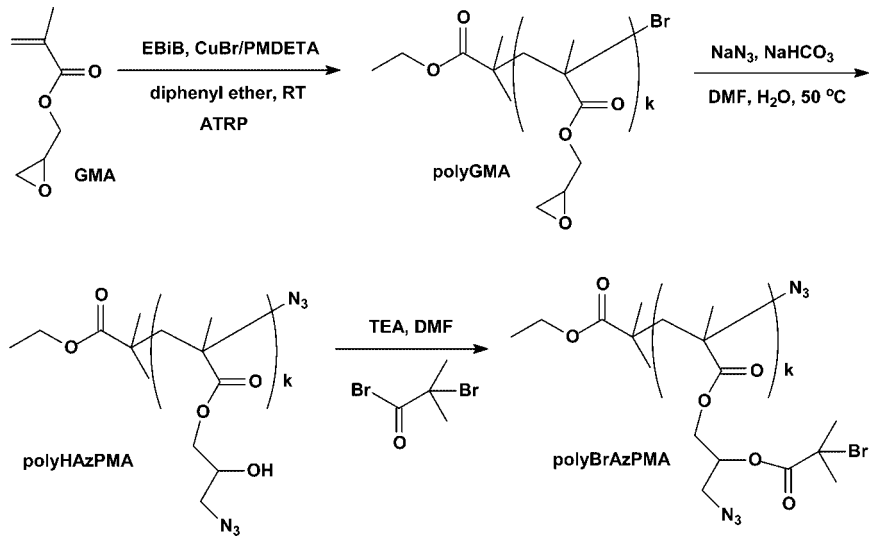

[a] GMA: glycidyl methacrylate, EBiB: ethyl 2-bromoisobutyrate, PMDETA: *N*,*N*,*N*′,*N*″,*N*″-pentmethyldiethylenetriamine, RT: room temperature, ATRP: atom transfer radical polymerization, TEA: triethylamine.

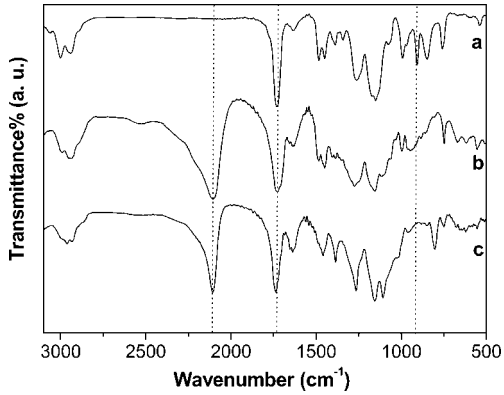

Figure 2. FTIR spectra of (a) poly(glycidyl methacrylate) (polyGMA), (b) poly(2-hydroxy-3-azidopropyl methacrylate) (polyHAzPMA), and (c) poly(3-azido-2-(2-bromo-2-methylpropanoyloxy)propyl methacrylate) (polyBrAzPMA).

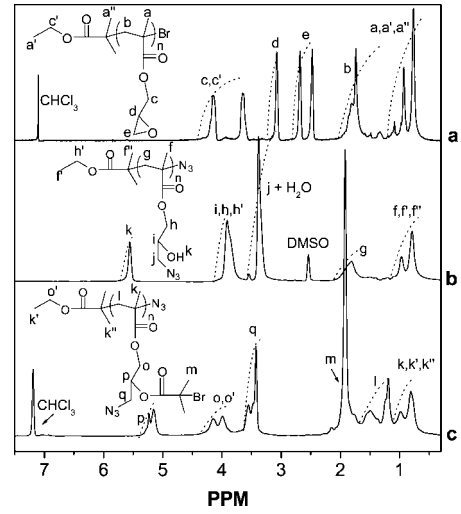

Figure 3. ^{1}H NMR (400 MHz) spectra of (a) poly(glycidyl methacrylate) (polyGMA), (b) poly(2-hydroxy-3-azidopropyl methacrylate) (polyHAzPMA), and (c) poly(3-azido-2-(2-bromo-2-methylpropanoyloxy)propyl methacrylate) (polyBrAzPMA).

each other because of the different side chains and (2) the hydrodynamic volumes of different polymers are different from each other. Our result of molecular weight change between polyHAzPMA and polyGMA is similar to that reported by Matyjaszewski et al. for the copolymer of GMA and methyl methacrylate (MMA), where M_n of the oxirane-ring-opened copolymer of poly(HAzPMA-*co*-MMA) was increased to 1.2 times that of its precursor poly(GMA-*co*-MMA).[26] In our case, M_n of homopolymer polyHAzPMA is about 1.3 times that of its precursor polymer polyGMA. After esterification of hydroxyl groups of polyHAzPMA with 2-bromoisobutyryl bromide, the M_n of polyBrAzPMA rose to 52 000, which is about 1.4 times that of its precursor polyHAzPMA. This phenomenon seems to be different from the case of pentynoic-acid-esterified poly(2-hydroxyethyl methacrylate) (PHEMA-alkyne) reported by Matyjaszewski et al., where M_n of PHEMA-alkyne was similar to that of its precursor PHEMA because the apparent M_n of PHEMA is considerably higher than its theoretical value as a result of the different hydrodynamic volumes between PHEMA and PMMA standards.[73] It is noteworthy that the clickable macroinitiator polyBrAzPMA itself is a good backbone for synthesizing cylindrical polymer brushes with bifunctional/Janus polymeric side chains, which will be demonstrated in our forthcoming work.

Growing Amphiphilic Polymer Brushes on Carbon Nanotubes. To graft clickable macroinitiators on the surfaces of CNTs using the Cu(I)-catalyzed click reaction of Huisgen 1,3-dipolar cycloaddition between azides and alkynes,[16] alkyne-functionalized CNTs (MWNT-Alk or SWNT-Alk) were first fabricated via two distinct ways, as described in the Experimental Section and Scheme 1. After the clickable macroinitiators were coated, we schemed two inverted methods for growing amphiphilic polymer brushes on CNTs. For MWNTs, we planned to grow hydrophobic polymer brushes of PnBMA first by in situ ATRP, followed by grafting hydrophilic polymer brushes of PEG-Alk on the surfaces via click chemistry. For SWNTs, we intended to first graft hydrophilic polymer brushes of PEG-Alk on the surfaces via click chemistry; then, hydrophobic polymer brushes of PS were introduced by in situ ATRP. The structures of the resulting functionalized CNTs were characterized and confirmed by TGA, FTIR, Raman, XPS, SEM, and TEM measurements.

TGA Measurements. Figure 5 displays the corresponding TGA weight-loss curves. The weight losses of pristine MWNTs and SWNTs below 550 °C are less than 1 and 5%, respectively.

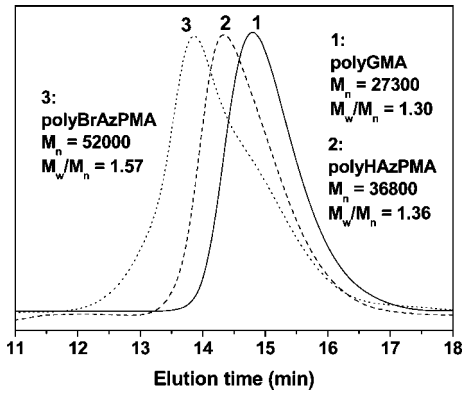

Figure 4. Gel permeation chromatography (GPC) elution curves of (1) poly(glycidyl methacrylate) (polyGMA), (2) poly(2-hydroxy-3-azidopropyl methacrylate) (polyHAzPMA), and (3) poly(3-azido-2-(2-bromo-2-methylpropanoyloxy)propyl methacrylate) (polyBrAzPMA).

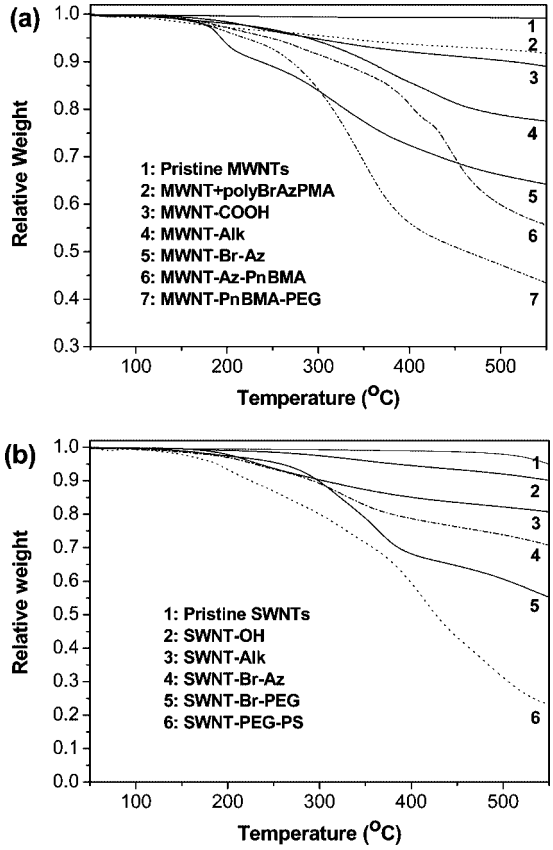

Figure 5. (a) Thermal gravimetric analysis (TGA) curves of (1) pristine multiwalled carbon nanotubes (MWNTs), (2) sample obtained from the control reaction between pristine MWNTs and poly(3-azido-2-(2-bromo-2-methylpropanoyloxy)propyl methacrylate) (polyBrAzPMA), (3) carboxyl-functionalized MWNTs (MWNT-COOH), (4) alkyne-modified MWNTs (MWNT-Alk), (5) MWNT-based clickable macroinitiator with both kinds of bromo and azido groups (MWNT-Br-Az), (6) poly(*n*-butyl methacrylate)-grafted MWNTs with azido groups (MWNT-Az-PnBMA), and (7) MWNTs grafted with both poly(*n*-butyl methacrylate) and poly(ethylene glycol) brushes (MWNT-PnBMA-PEG). (b) TGA curves of (1) pristine single-walled carbon nanotubes (SWNTs), (2) hydroxyl-group-functionalized SWNTs (SWNT-OH), (3) alkyne-modified SWNTs (SWNT-Alk), (4) SWNT-based clickable macroinitiator (SWNT-Br-Az), (5) poly(ethylene glycol)-brushes-grafted SWNTs with alkyl bromo groups (SWNT-Br-PEG), and (6) SWNTs grafted with both poly(ethylene glycol) and poly(styrene) brushes (SWNT-PEG-PS).

In the case of MWNT-COOH and MWNT-Alk fabricated by acylation between as-prepared acyl-chloride-functionalized

Table 1. Growing Amphiphilic Polymer Brushes on Multiwalled Carbon Nanotube (MWNT) Surfaces via a Combination of Click Chemistry and Macroinitiator Approach

sample	MWNT-Br-Az mg/mmol	[I]/[Cu(I)]/[L]/[M]	PEG-Alk mg/mg[a]	f_{wt} %[b]	inc %[c]
MWNT-COOH				10.9	
MWNT-Alk				22.5	16.8
MWNT-Br-Az				35.8	26.7
MWNT-Az-PnBMA	50/0.0193	1:2:2:250		44.3	23.8
MWNT-PnBMA-PEG			1:10	56.4	49.8

[a] Mass ratio of MWNT-Az-PnBMA to PEG-Alk. [b] Weight fraction of grafted polymer calculated from TGA results. [c] Relative increment compared with the corresponding precursor with the same number of neat CNTs.

Table 2. Growing Amphiphilic Polymer Brushes on Single-Walled Carbon Nanotube (SWNT) Surfaces via a Combination of Click Chemistry and Macroinitiator Approach

sample	SWNT-Br-PEG mg/mmol	[I]/[Cu(I)]/[L]/[M]	PEG-Alk mg/mg[a]	f_{wt} %[b]	inc %[c]
SWNT-OH				9.9	
SWNT-Alk				19.3	12.9
SWNT-Br-Az				29.3	17.5
SWNT-Br-PEG			1:10	44.8	39.7
SWNT-PEG-PS	25/0.0072	1:2:2:500		76.8	249.9

[a] Mass ratio of SWNT-Br-Az/PEG-Alk. [b] Weight fraction of grafted polymer calculated from TGA results. [c] Relative increment compared with the corresponding precursor with the same number of neat CNTs.

MWNTs and propargyl alcohol, the weight losses are 10.9 and 22.5%, respectively. Estimated from the results, the density of alkyne groups on the surfaces of MWNT-Alk is ~2.71 mmol per gram of MWNT-Alk. After grafting clickable macroinitiators on MWNTs, there is a definite decomposition stage below 210 °C for MWNT-Br-Az. It is assumed that the decomposition of residual azido groups (confirmed by FTIR observation) caused the weight-loss at a relatively low temperature. After growing two different polymer brushes on MWNTs, the weight losses increased to 44.3 and 56.4%, respectively. As for SWNTs series, we applied a different way of synthesizing hydroxyl-functionalized SWNTs (SWNT-Alk) via the addition of nitrene formed by thermolysis of 2-azidoethanol to strained double bonds of SWNTs. Alkyne groups were introduced by an acylation reaction between acyl chloride groups derived from as-prepared 4-oxo-4-(prop-2-ynyloxy)butanoic acid and hydroxyl groups of SWNT-OH. The weight losses of SWNT-OH and SWNT-Alk below 550 °C are 9.9 and 19.3%, respectively, corresponding to 0.76 mmol alkyne groups per gram of SWNT-Alk. The weight loss of SWNT-Br-Az increased to 29.3%, which indicated that polyBrAzPMA was immobilized on SWNTs. After PEG-Alk brushes were grafted to and PS brushes were grafted from SWNTs, the weight losses increased to 44.8 and 76.8%, respectively, implying the effective grafting efficiency for both click reaction and ATRP. The results are also summarized in Tables 1 and 2. Radical coupling reaction between the bromo groups and the π bonds of CNT surfaces may occur to graft the macroinitiator directly onto CNTs in the presence of CuBr/PMDETA.[3] To check the competing ability of the radical coupling, we carried out the control experiment of the reaction between pristine MWNTs instead of MWNT-Alk and polyBrAzPMA. Less than 8% weight loss was observed in the corresponding TGA curve (Figure 5a), indicating that the radical coupling reaction was much less efficient than the click reaction that permitted a grafting efficiency of 26.7 wt %. Therefore, the predominant reaction between MWNT-Alk and polyBrAzPMA would be click coupling.

From the results of TGA, we can conclude that (1) the two functional groups (azide groups for click reaction and alkyl bromo groups for ATRP reaction) are compatible and both of them have high reactivity after binding on CNTs, (2) it is feasible and discretionary to grow polymer brushes via the

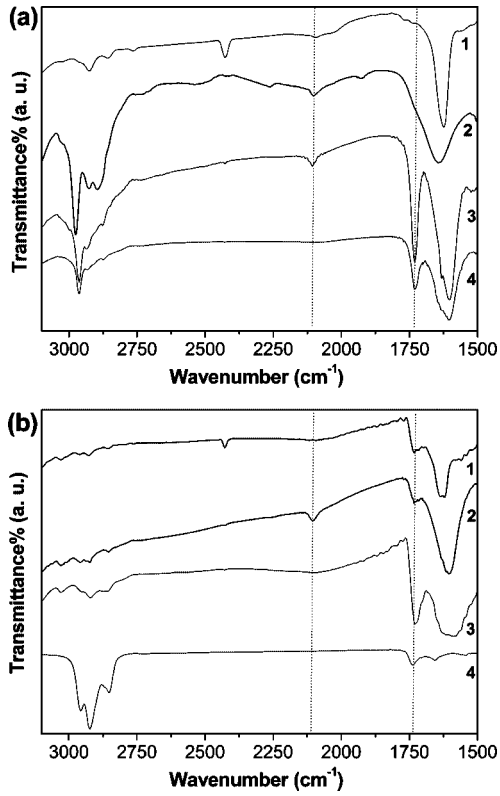

Figure 6. (a) FTIR spectra of (1) alkyne-modified multiwalled carbon nanotubes (MWNT-Alk), (2) MWNT-based clickable macroinitiator with both kinds of bromo and azido groups (MWNT-Br-Az), (3) poly(*n*-butyl methacrylate)-grafted MWNTs with azido groups (MWNT-Az-PnBMA), and (4) MWNTs grafted with both poly(*n*-butyl methacrylate) and poly(ethylene glycol) brushes (MWNT-PnBMA-PEG). (b) FTIR spectra of (1) alkyne-modified single-walled carbon nanotubes (SWNT-Alk), (2) SWNT-based clickable macroinitiator (SWNT-Br-Az), (3) poly(ethylene glycol)-grafted SWNTs with bromo groups (SWNT-Br-PEG), and (4) SWNTs grafted with both poly(ethylene glycol) and polystyrene brushes (SWNT-PEG-PS).

grafting to first or the grafting from first approach, and (3) different types of polymer brushes can grow on CNTs by a combination of click chemistry and in situ ATRP.

FTIR, Raman, and XPS Spectra. As displayed in Figure 6a, the characteristic absorption signals of carbonyl band at around 1730 cm^{-1} are hardly detected for MWNT-Alk and MWNT-Br-Az, but the appearance of the characteristic absorption of azido groups at ca. 2102 cm^{-1} indicates that polyBrAz-PMA has been coated on the MWNT-Alk via click reaction and that there is still a number of residual azido groups on the surface of MWNTs. After PnBMA brushes grew on MWNTs, the intensity of the carbonyl band increased remarkably and the characteristic absorption of azido groups remained. As expected, the characteristic absorption of azido groups disappeared after PEG-Alk brushes were clicked to the MWNT-Az-PnBMA. These results indicated that ATRP reaction that was initiated by alkyl bromo groups will not intervene in the subsequent click reaction.

In the case of SWNTs, as shown in Figure 6b, the characteristic absorption signal at ca. 1730 cm^{-1} is clearly observed for SWNT-Alk, which can be attributed to the carbonyl band that originated from 4-oxo-4-(prop-2-ynyloxy)butanoic acid. A new peak at ~2104 cm^{-1} was found for SWNT-Br-Az and was assigned to the absorption of azido groups, indicating that polyBrAzPMA had been successfully coated on the SWNT-Alk. The peak of azido groups was no longer observed for SWNT-Br-PEG, and the intensity of the carbonyl band increased considerably because of the introduction of the carbonyl band

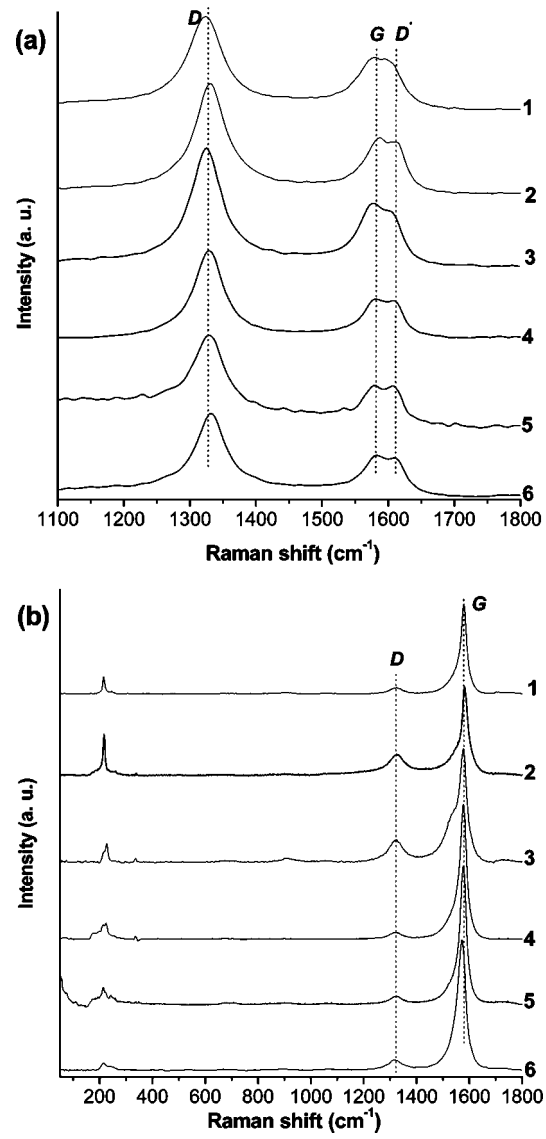

Figure 7. (a) Raman spectra of (1) pristine multiwalled carbon nanotubes (MWNTs), (2) carboxyl-functionalized MWNTs (MWNT-COOH), (3) alkyne-modified MWNTs (MWNT-Alk), (4) MWNT-based clickable macroinitiator with both kinds of bromo and azido groups (MWNT-Br-Az), (5) poly(*n*-butyl methacrylate)-grafted MWNTs with azido groups (MWNT-Az-PnBMA), and (6) MWNTs grafted with both poly(*n*-butyl methacrylate) and poly(ethylene glycol) brushes (MWNT-PnBMA-PEG). (b) Raman spectra of (1) pristine single-walled carbon nanotubes (SWNTs), (2) hydroxyl-group-functionalized SWNTs (SWNT-OH), (3) alkyne-modified SWNTs (SWNT-Alk), (4) SWNT-based clickable macroinitiator (SWNT-Br-Az), (5) poly(ethylene glycol)-grafted SWNTs with alkyl bromo groups (SWNT-Br-PEG), and (6) SWNTs grafted with both poly(ethylene glycol) and poly(styrene) brushes (SWNT-PEG-PS).

(O═CCH_2CH_2C═O) of PEG-Alk. This confirms that it is highly efficient to graft PEG-Alk brushes to SWNT-Br-Az, which contained residual azido groups. The grown PS brushes were characterized with peaks of very strong intensity at ca. 2922 and 2852 cm^{-1} (the stretching of C−H of PS brushes), and the intensity of the carbonyl band decreased. The results declare that the first-performed click reaction will not intervene in the sequential ATRP reaction.

The Raman spectra for crude CNTs and functionalized CNTs are shown in Figure 7. For all MWNT samples (Figure 7a), the D and G bands at ca. 1327 and 1581 cm^{-1} were clearly detected and are associated with the defects/disorder-induced modes and the vibration of sp^2-bonded carbon atoms in a 2D hexagonal

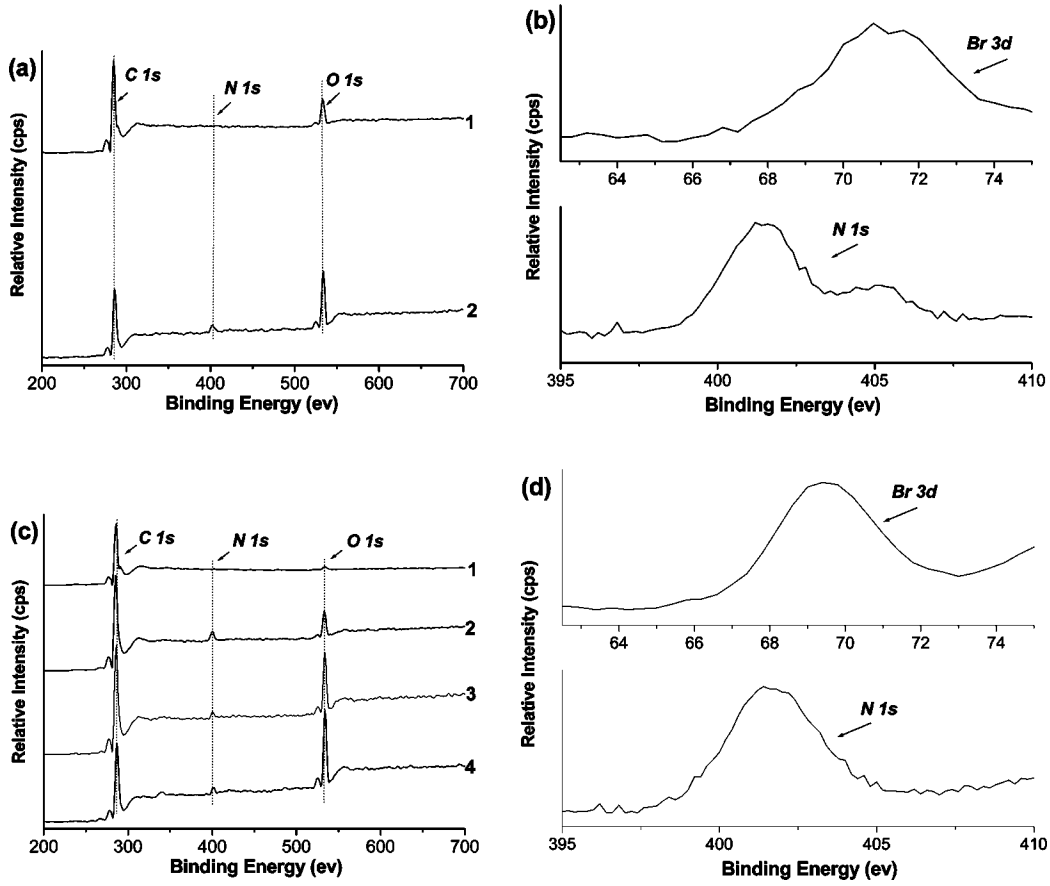

Figure 8. (a) XPS spectra of (1) alkyne-modified multiwalled carbon nanotubes (MWNT-Alk) and (2) MWNT-based clickable macroinitiator with both kinds of bromo and azido groups (MWNT-Br-Az). (b) XPS spectra for the N (1s) and Br (3d) region of MWNT-Br-Az. (c) XPS spectra of (1) pristine single-walled carbon nanotubes (SWNTs), (2) hydroxyl groups functionalized SWNTs (SWNT-OH), (3) alkyne-modified SWNTs (SWNT-Alk), and (4) SWNT-based clickable macroinitiator (SWNT-Br-Az). (d) XPS spectra for the N (1s) and Br (3d) region of SWNT-Br-Az.

Table 3. Mole Content of Bromine and Nitrogen Obtained from XPS and TGA Results

sample	Br/C%[a]	N/C%[b]	$Br_{xps} \times 10^3$ mol/g[c]	$N_{xps} \times 10^3$ mol/g[d]	$Br_{TGA} \times 10^3$ mol/g[e]	$N_{TGA} \times 10^3$ mol/g[f]
MWNT-Alk	0	0.70	0	0.50	0	0
MWNT-Br-Az	2.12	7.41	1.02	3.59	0.51	1.56
SWNT-OH	0	6.45	0	4.44	0	1.68
SWNT-Alk	0	4.08	0	2.59	0	1.50
SWNT-Br-Az	1.06	5.95	0.573	3.21	0.32	2.43

[a] Relative atomic ratios of bromine to carbon derived from quantitative XPS analysis. [b] Relative atomic ratios of nitrogen to carbon derived from quantitative XPS analysis. [c] Mole content of bromine on the surface of CNTs derived from quantitative XPS analysis. [d] Mole content of nitrogen on the surface of CNTs derived from quantitative XPS analysis. [e] Mole content of bromine calculated from TGA results. [f] Mole content of nitrogen calculated from TGA results.

lattice, respectively.[87,88] The ratios of D- to G-band intensity (I_D/I_G) exhibit the degree of disorder in MWNTs.[87,88] The values of I_D/I_G for MWNT-COOH (1.97) and MWNT-Alk (1.88) are greater than that of pristine MWNTs (ca. 1.62), which indicates the increase in defects in MWNTs due to the chemical functionalization. The D′ band at ~1610 cm^{-1}, which is also attributed to the defects and disorder in MWNTs, can hardly be found for pristine MWNTs, whereas it is clearly observed for all of the functionalized MWNTs, which also indicates the defects of MWNTs enhanced after functionalization. Characteristic Raman signals of grafted polymers were not found, which is consistent with our previously reported results of covalent functionalization of CNTs.[47]

For the samples of SWNTs, as displayed in Figure 7b, the characteristic radial breathing mode (RBM) around 160−280 cm^{-1}, D band at ca. 1319.0 cm^{-1}, and G band at ca. 1582.0 cm^{-1} were observed clearly and are assigned to the symmetric movement of all carbon atoms in the radial direction, disorder mode, and tangential mode,[89] respectively. For SWNT-OH (I_D/I_G = 0.237), the relative intensity of the D band markedly increased compared with that of the pristine SWNTs (I_D/I_G = 0.067), which confirmed the covalent modification of pristine SWNTs via nitrene addition. The sequential funtionalizations of SWNT-Alk did not result in the obvious increase in the D-band intensity, which likely because the polymer was not directly linked on the carbons of CNTs. Similar phenomena have been previously reported.[27]

XPS analysis was applied as another powerful tool for determining the surface compositions of functionalized CNTs. Figure 8a displays the whole XPS spectra of MWNT-Alk and MWNT-Br-Az. Signals at about 285.0 (C1s) and 533.0 eV (O1s) are clearly detected for both samples. A new peak at 402.0 eV that corresponds to the N1s region was observed for MWNT-Br-Az, which supports the fact that polyBrAzPMA has been clicked on MWNT-Alk. In addition, the narrow scan spectrum of MWNT-Br-Az (Figure 8b) shows the absorption of Br 3d at ~70.8 eV and two distinct peaks at 401 and 405 eV, respectively. The 405 eV peak with higher binding energy is attributed to the relatively electron-poor middle N atom of the azido

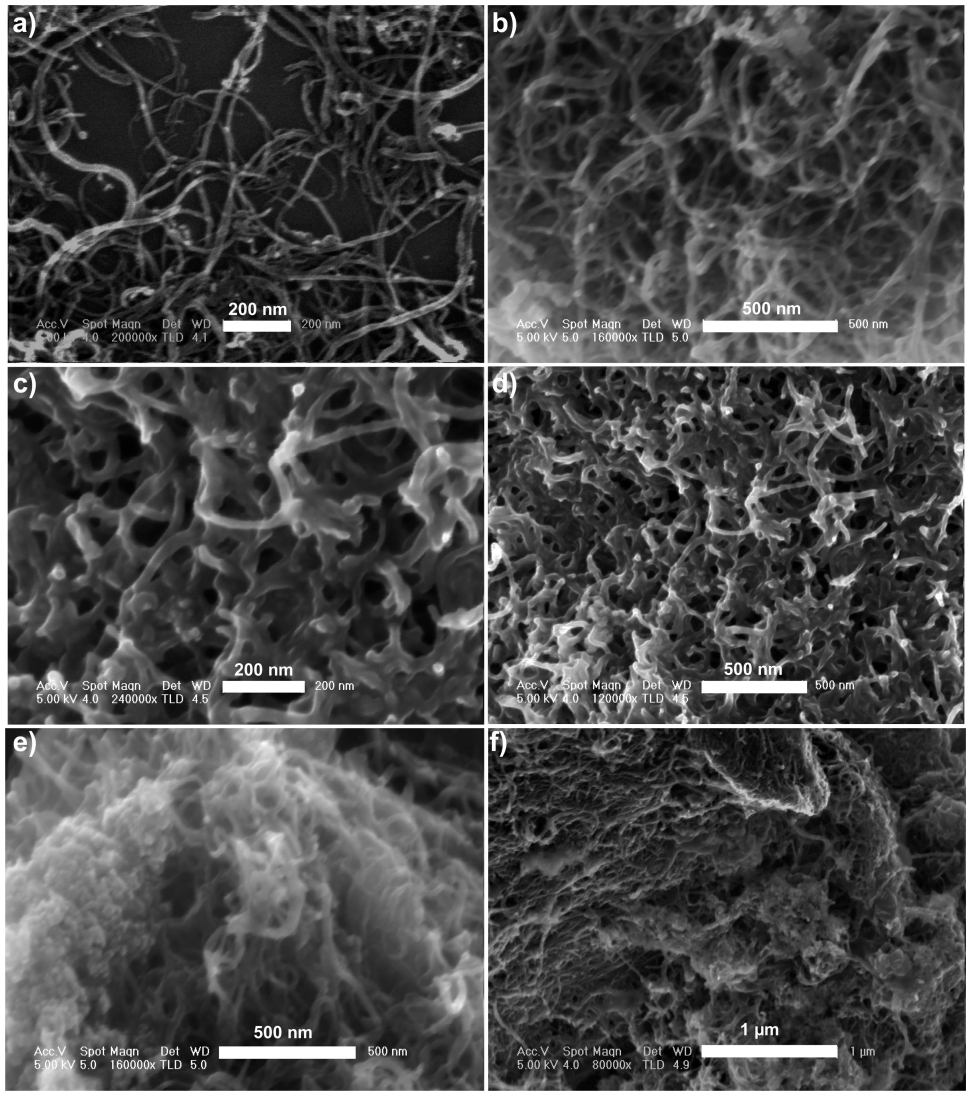

Figure 9. Representative SEM images of (a) alkyne-modified multiwalled carbon nanotubes (MWNT-Alk), (b) MWNT-based clickable macroinitiator (MWNT-Br-Az), (c,d) poly(*n*-butyl methacrylate)-grafted MWNTs with azido groups (MWNT-Az-PnBMA), and (e,f) MWNTs grafted with both poly(*n*-butyl methacrylate) and poly(ethylene glycol) brushes (MWNT-PnBMA-PEG).

group,[90] which indicates that a large number of azido groups exist on the surfaces of MWNT-Br-Az.

The whole XPS spectra of pristine SWNTs, SWNT-OH, SWNT-Alk, and SWNT-Br-Az are shown in Figure 8c. Only one peak at ca. 285.0 eV (C1s) was found for pristine SWNTs. After the addition between nitrene and pristine SWNTs, two peaks appeared at 400.0 (N1s) and 533.0 eV (O1s), respectively. The results demonstrated that hydroxyl groups were introduced to the surface of SWNTs via the radical coupling approach. For SWNT-Alk, the intensity of the O1s peak increased with respect to the peak of C1s, which is attributed to the introduction of oxygen atoms ($O{=}CCH_2CH_2C{=}OO$) of 4-oxo-4-(prop-2-ynyloxy)butanoic acid. Peaks at about 287.0 (C1s), 401.0 (N1s), and 534.0 eV (O1s) are also clearly observed for SWNT-Br-Az. In the narrow scan spectrum of SWNT-Br-Az (Figure 8d), the absorption of Br 3d at ~69.4 eV was observed, and only one peak appeared at 401.4 eV (N1s), which is likely due to the relatively low density of polyBrAzPMA coated on SWNT-Alk and the consumption of part of the azido groups during the click reaction. The XPS results further demonstrate the formation of a CNT-based clickable macroinitiator with essential azido and bromo groups. Quantitative analyses were also carried out to compare the relative atomic ratio of the CNTs before and after functionalization. For the sample of MWNT-Br-Az, the relative atomic ratio of N/C (7.41%) is about three times greater than that of Br/C (2.12%), which is in accordance with the theoretical N/Br ratio of approximately 3:1. As for SWNT-OH synthesized via the addition of nitrene to strained double bonds of SWNTs, the N/C ratio increases to 6.45%, which is more than one order of magnitude higher than that of pristine SWNTs (0.29%). After polyBrAzPMA was clicked to SWNT-Alk, the relative atomic ratio of N/C increased from 4.08% for SWNT-Alk to 5.95% for SWNT-Br-Az. The relative atomic ratio of Br/C for SWNT-Br-Az is 1.06%, which is about one-sixth as great as that of N/C. The low Br/N ratio can be attributed to the presence of nitrogen in the material of SWNT-OH. The mole contents of bromine and nitrogen derived from XPS are higher than the results calculated from TGA weight-loss data (summarized in Table 3), which is likely due to the fact that XPS can more accurately detect the surface element distribution of nanoobjects, and TGA can detect the whole organic moieties immobilized on CNTs.

SEM and TEM Observations. The structure and morphology of the resultant samples were observed by SEM. Figure 9a shows a typical image of MWNT-Alk. A smooth nanowirelike morphology was found. For the sample of MWNT-Br-Az (Figure 9b), the space among MWNTs becomes smaller, but

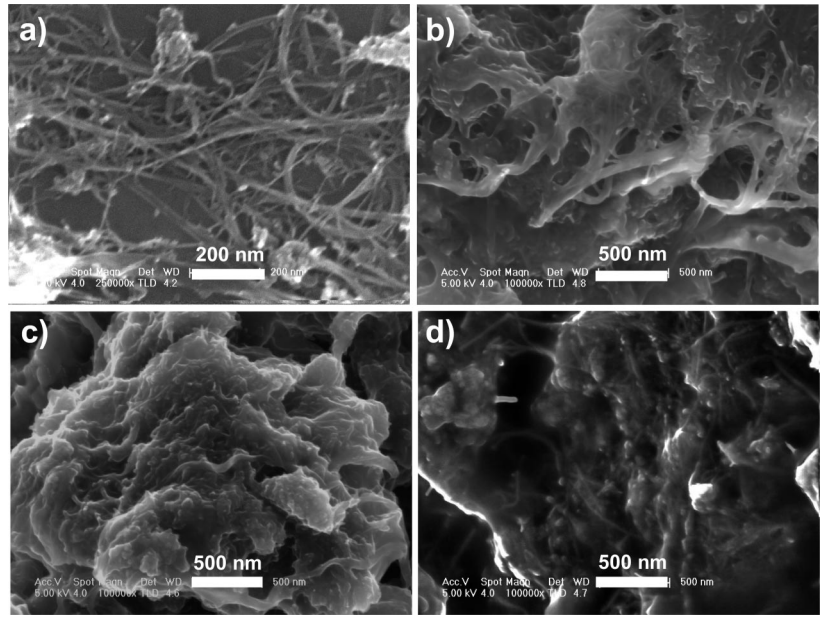

Figure 10. Representative SEM images of (a) alkyne-modified single-walled carbon nanotubes (SWNT-Alk), (b) SWNT-based clickable macroinitiator (SWNT-Br-Az), (c) poly(ethylene glycol)-grafted SWNTs with alkyl bromo groups (SWNT-Br-PEG), and (d) SWNTs grafted with both poly(ethylene glycol) and poly(styrene) brushes (SWNT-PEG-PS).

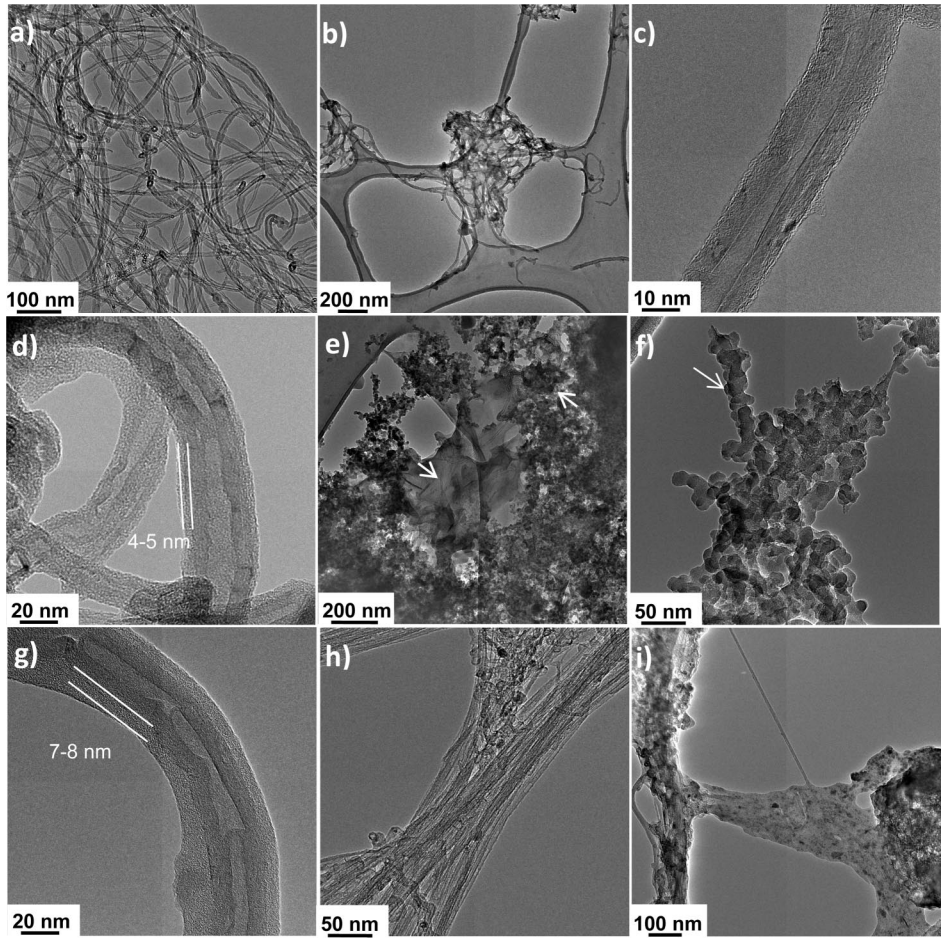

Figure 11. Representative TEM images of (a) pristine multiwalled carbon nanotubes (MWNTs), (b,c) MWNT-based clickable macroinitiator (MWNT-Br-Az), (d) poly(*n*-butyl methacrylate)-grafted MWNTs with azido groups (MWNT-Az-PnBMA), (e−g) MWNTs grafted with both poly(*n*-butyl methacrylate) and poly(ethylene glycol) brushes (MWNT-PnBMA-PEG), (h) hydroxyl-group-functionalized single-walled carbon nanotubes (SWNT-OH), and (i) SWNTs grafted with both poly(ethylene glycol) and poly(styrene) brushes (SWNT-PEG-PS).

no continuous polymer phase was observed because of the relatively low degree of grafting. As for the sample of MWNT-Az-PnBMA (Figure 9c,d), the space among MWNTs becomes even smaller, and a nanowirelike morphology becomes more continuous because of the PnBMA brushes grown on the surfaces. For the sample of MWNT-PnBMA-PEG (Figure 9e,f)

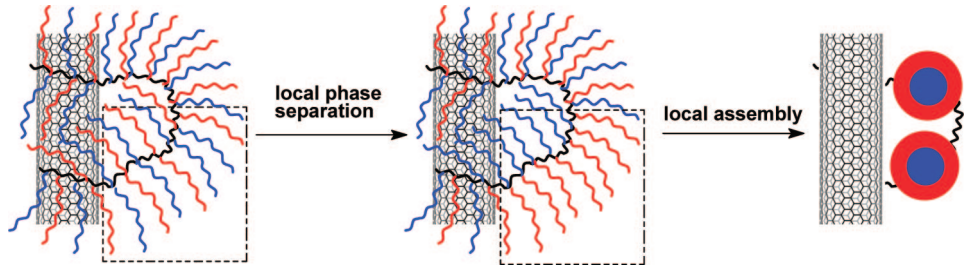

Figure 12. Cartoon of the local phase separation and assembly of amphiphilic polymer brushes into Janus polymer structures on carbon nanotubes.

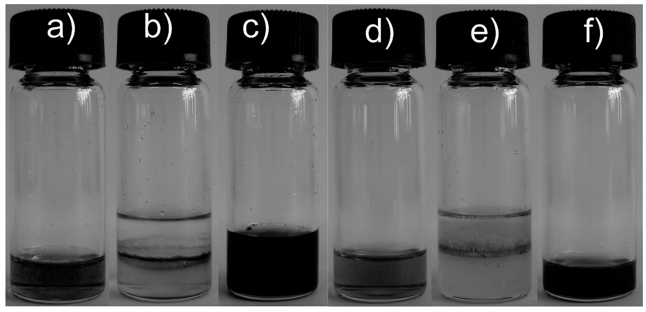

Figure 13. Photographs of the solubility/dispersibility behavior of modified CNTs: (a) multiwalled carbon nanotubes grafted with both poly(*n*-butyl methacrylate) and poly(ethylene glycol) brushes (MWNT-PnBMA-PEG) in chloroform, (b) MWNT-PnBMA-PEG in a mixed solvent of water (upper layer) and chloroform (bottom layer), (c) poly(*n*-butyl methacrylate)-grafted MWNTs (MWNT-Az-PnBMA) in chloroform, (d) single-walled carbon nanotubes grafted with both poly(ethylene glycol) and poly(styrene) brushes (SWNT-PEG-PS) in chloroform, (e) SWNT-PEG-PS in a mixed solvent of water (upper layer) and chloroform (bottom layer), and (f) poly(ethylene glycol)-grafted SWNTs (SWNT-Br-PEG) in water.

grafted with both PnBMA and PEG brushes, a continuous polymer phase was observed, and rodlike MWNTs were found protruding through polymer layers.

Similar morphology was observed for the samples of SWNTs (Figure 10). The SEM image of SWNT-Alk shows the morphology of small bundles, which are aggregated by individual SWNT tubes (Figure 10a). Generally, with increasing content of polymer via either the grafting to or the grafting from approach, the distances between SWNT tubes become smaller and the phase of polymer become more continuous. For the sample of SWNT-PEG-PS with the highest polymer content, the polymer phase dominates the overall morphology, and SWNTs are fully enwrapped by polymer chains.

The fine structures of resulting samples were also characterized by TEM. For comparison, the TEM image of pristine MWNT is displayed, showing a tubular structure with a smooth and clean surface (Figure 11a). After polyBrAzPMA was clicked to the surfaces of MWNT-Alk, the nanotubes were clearly observed and well-dispersed under lower magnification (Figure 11b). Under higher magnification, the surfaces of the sample look hairy and coarse (Figure 11c). Figure 11d shows the TEM image of MWNT-Az-PnBMA under high magnification. A distinct core−shell structure with MWNT at the center was clearly observed, and the thickness of the polymer layer was about 4 to 5 nm. In the low-resolution image for the sample of MWNT-PnBMA-PEG (Figure 11e), it is found that MWNT was fully covered with polymers. Interestingly, under higher magnification (Figure 11f), some protuberance- and bead-like structures were observed. This may be ascribed to the existence and local aggregation of extended amphiphilic polymer brushes in Janus polymer structures on CNT surfaces, as illustrated in Figure 12. An isolated core−shell nanotube of MWNT-PnBMA-PEG is shown in Figure 11g, and the thickness of the polymer shell increased considerably to ca. 7 to 8 nm. Figure 11h shows the TEM image of SWNT-OH. It is found that individual SWNTs aggregate in large bundles with a diameter of dozens of nanometers. After growing two kinds of polymer brushes, the SWNTs were fully enwrapped by polymer layers, and nanowirelike SWNTs could hardly be found (Figure 11i).

Solubility Behavior of Carbon Nanotubes (CNTs) Functionalized with Amphiphilic/Janus Polymer Brushes. As expected, both MWNT-PnBMA-PEG and SWNT-PEG-PS grafted with amphiphilic/Janus polymer brushes were soluble/dispersible in chloroform (Figure 13a,d) and underwent self-assembly at the chloroform/water interface to form a special film (Figure 13b,e), which is similar to the previously reported phenomenon for the core−shell amphiphilic CNTs.[91] This indicates that amphiphilic polymer brushes could form Janus structures at the oil/water interface by self-aggregation of the same polymer phase. In addition, the PnBMA-brushes-grafted MWNTs (MWNT-Az-PnBMA) and poly(ethylene glycol)-brushes-grafted SWNTs (SWNT-Br-PEG) displayed good dispersibility in chloroform and water (Figure 13c,f), respectively, which is in agreement with their corresponding hydrophobic and hydrophilic characters.

Conclusions

A novel Gemini-grafting strategy for modifying surfaces has been presented and demonstrated with CNTs as a kind of model surface and with click chemistry and ATRP as "grafting to" and "grafting from" techniques, respectively. The Gemini-grafting strategy shows various advantages: (1) the generality that allows it can be extended to modify any other planar, globular, or topologically complex substrate/surface, (2) the simplicity of procedures and processes that results in scalable fabrication of functionalized surfaces, (3) the high efficiency that makes a high density of polymer grafting readily realizable, (4) the versatility that promises multifunctions of different polymers can be easily integrated onto a surface, and (5) the controllability of the quantity and sort of grafted polymers. The key step of the Gemini-grafting strategy lies in the preparation of the macroinitiator with different kinds of functional groups. Therefore, both organic reactions and polymerization techniques can be used to design the macroinitiator according to specific requirements, opening a new era of multifunctional surfaces, hybrid materials, and polymer brushes. The extension of substrates and polymerizations is in progress and will be later reported.

Acknowledgment. This work was financially supported by the National Natural Science Foundation of China (no. 50773038), the National Basic Research Program of China (973 Program) (no. 2007CB936000), the Science and Technology Commission of Shanghai Municipality (07pj14048), the Program for New Century Excellent Talents in University of China, and the Foundation for

the Author of National Excellent Doctoral Dissertation of China (no. 200527).

Supporting Information Available: ^{1}H NMR spectrum of 4-oxo-4-(prop-2-ynyloxy)butanoic acid and ^{1}H NMR spectra of polyGMA, polyHAzPMA, and polyBrAzPMA with integration values. This material is available free of charge via the Internet at http://pubs.acs.org.

References and Notes

(1) Kong, H.; Luo, P.; Gao, C.; Yan, D. *Polymer* **2005**, *46*, 2472–2485.
(2) Ranjan, R.; Brittain, W. J. *Macromolecules* **2007**, *40*, 6217–6223.
(3) Liu, Y.-L.; Chen, W.-H. *Macromolecules* **2007**, *40*, 8881–8886.
(4) Lyatskaya, Y.; Balazs, A. C. *Macromolecules* **1998**, *31*, 6676–6680.
(5) Edmondson, S.; Osborne, V. L.; Huck, W. T. S. *Chem. Soc. Rev.* **2004**, *33*, 14–22.
(6) Radhakrishnan, B.; Ranjan, R.; Brittain, W. J. *Soft Matter* **2006**, *2*, 386–396.
(7) Advincula, R. *Adv. Polym. Sci.* **2006**, *197*, 107–136.
(8) Tsujii, Y.; Ohno, K.; Yamamoto, S.; Goto, A.; Fukuda, T. *Adv. Polym. Sci.* **2006**, *197*, 1–45.
(9) Chen, X.; Armes, S. P. *Adv. Mater.* **2003**, *15*, 1558–1562.
(10) Edmondson, S.; Vo, C.-D.; Armes, S. P.; Unali, G.-F.; Weir, M. P. *Langmuir* **2008**, *24*, 7208–7215.
(11) Wang, J.; Matyjaszewski, K. *J. Am. Chem. Soc.* **1995**, *117*, 5614–5615.
(12) Wang, J.; Matyjaszewski, K. *Macromolecules* **1995**, *28*, 7572–7573.
(13) Matyjaszewski, K.; Xia, J. *Chem. Rev.* **2001**, *101*, 2921–2990.
(14) *Handbook of Radical Polymerization*; Matyjaszewski, K., Davis, T. P., Eds.; Wiley: Hoboken, NJ, 2002.
(15) Tsarevsky, N. V.; Matyjaszewski, K. *Chem. Rev.* **2007**, *107*, 2270–2299.
(16) Kolb, H. C.; Finn, M. G.; Sharpless, K. B. *Angew. Chem., Int. Ed.* **2001**, *40*, 2004–2021.
(17) Rostovtsev, V. V.; Green, L. G.; Fokin, V. V.; Sharpless, K. B. *Angew. Chem., Int. Ed.* **2002**, *41*, 2596–2599.
(18) Kolb, H. C.; Sharpless, B. K. *Drug Discovery Today* **2003**, *8*, 1128–1137.
(19) Wolfbeis, O. S. *Angew. Chem., Int. Ed.* **2007**, *46*, 2980–2982.
(20) Binder, W. H.; Sachsenhofer, R. *Macromol. Rapid Commun.* **2007**, *28*, 15–54.
(21) Lutz, J. F.; Borner, H. G. *Prog. Polym. Sci.* **2008**, *33*, 1–39.
(22) Acar, M. H.; Matyjaszewski, K. *Macromol. Chem. Phys.* **1999**, *200*, 1094–1100.
(23) Gao, C.; Vo, C. D.; Jin, Y. Z.; Li, W.; Armes, S. P. *Macromolecules* **2005**, *38*, 8634–8648.
(24) Sumerlin, B. S.; Tsarevsky, N. V.; Louche, G.; Lee, R. Y.; Matyjaszewski, K. *Macromolecules* **2005**, *38*, 7540–7545.
(25) Krishnan, R.; Srinivasan, K. S. V. *Macromolecules* **2003**, *36*, 1769–1771.
(26) Tsarevsky, N. V.; Bencherif, S. A.; Matyjaszewski, K. *Macromolecules* **2007**, *40*, 4439–4445.
(27) Qin, S.; Qin, D.; Ford, W. T.; Resasco, D. E.; Herrera, J. E. *J. Am. Chem. Soc.* **2004**, *126*, 170–176.
(28) Kong, H.; Gao, C.; Yan, D. *Macromolecules* **2004**, *37*, 4022–4030.
(29) Iijima, S. *Nature* **1991**, *354*, 56–58.
(30) Ajayan, P. M. *Chem. Rev.* **1999**, *99*, 1787–1800.
(31) Tasis, D.; Tagmatarchis, N.; Bianco, A.; Prato, M. *Chem. Rev.* **2006**, *106*, 1105–1136.
(32) Monthioux, M. *Carbon* **2002**, *40*, 1809–1823.
(33) Ajayan, P. M.; Zhou, O. Z. *Top. Appl. Phys.* **2001**, *80*, 391–425.
(34) Lukaszewicz, J. P. *Sens. Lett.* **2006**, *4*, 53–98.
(35) Kahn, M. G. C.; Banerjee, S.; Wong, S. S. *Nano Lett.* **2002**, *2*, 1215–1218.
(36) Huang, W.; Fernando, S.; Allard, L. F.; Sun, Y.-P. *Nano Lett.* **2003**, *3*, 565–568.
(37) Lin, Y.; Zhou, B.; Fernando, K. A. S.; Allard, L. F.; Sun, Y.-P. *Macromolecules* **2003**, *36*, 7199–7204.
(38) Li, H. M.; Cheng, F. O.; Duft, A. M.; Adronov, A. *J. Am. Chem. Soc.* **2005**, *127*, 14518–14524.
(39) Liu, Y. Q.; Yao, Z. L.; Adronov, A. *Macromolecules* **2005**, *38*, 1172–1179.
(40) Lou, X. D.; Detrembleur, C.; Pagnoulle, C.; Jerome, R.; Bocharova, V.; Kiriy, A.; Stamm, M. *Adv. Mater.* **2004**, *16*, 2123–2127.
(41) Kitano, H.; Tachimoto, K.; Anraku, Y. *J. Colloid Interface Sci.* **2007**, *306*, 28–33.
(42) Wu, W.; Zhang, S.; Li, Y.; Li, J.; Liu, L.; Qin, Y.; Guo, Z.-X.; Dai, L.; Ye, C.; Zhu, D. *Macromolecules* **2003**, *36*, 6286–6288.
(43) Huang, H. M.; Liu, I. C.; Chang, C. Y.; Tsai, H. C.; Hsu, C. H.; Tsiang, R. C. C. *J. Polym. Sci., Part A: Polym. Chem.* **2004**, *42*, 5802–5810.
(44) Xu, H. X.; Wang, X. B.; Zhang, Y. F.; Liu, S. Y. *Chem. Mater.* **2006**, *18*, 2929–2934.
(45) Petrov, P.; Lou, X. D.; Pagnoulle, C.; Jerome, C.; Calberg, C.; Jerome, R. *Macromol. Rapid Commun.* **2004**, *25*, 987–990.
(46) Zeng, H. L.; Gao, C.; Wang, Y. P.; Watts, P. C. P.; Kong, H.; Cui, X. W.; Yan, D. Y. *Polymer* **2006**, *47*, 113–122.
(47) Gao, C.; Jin, Y. Z.; Kong, H.; Whitby, R. L. D.; Acquah, S. F. A.; Chen, G. Y.; Qian, H. H.; Hartschuh, A.; Silva, S. R. P.; Henley, S.; Fearon, P.; Kroto, H. W.; Walton, D. R. M. *J. Phys. Chem. B* **2005**, *109*, 11925–11932.
(48) Nogales, A.; Broza, G.; Roslaniec, Z.; Schulte, K.; Sics, I.; Hsiao, B. S.; Sanz, A.; Garcia-Gutierrez, M. C.; Rueda, D. R.; Domingo, C.; Ezquerra, T. A. *Macromolecules* **2004**, *37*, 7669–7672.
(49) Cui, J.; Wang, W. P.; You, Y. Z.; Liu, C. H.; Wang, P. H. *Polymer* **2004**, *45*, 8717–8721.
(50) Hong, C. Y.; You, Y. Z.; Pan, C. Y. *Chem. Mater.* **2005**, *17*, 2247–2254.
(51) Hong, C. Y.; You, Y. Z.; Pan, C. Y. *J. Polym. Sci., Part A: Polym. Chem.* **2006**, *44*, 2419–2427.
(52) You, Y. Z.; Hong, C. Y.; Pan, C. Y. *Nanotechnology* **2006**, *17*, 2350–2354.
(53) Dehonor, M.; Masenelli-Varlot, K.; González-Montiel, A.; Gauthier, C.; Cavaillé, J. Y.; Terrones, H.; Terrones, M. *Chem. Commun.* **2005**, 5349–5351.
(54) Zhao, X. D.; Fan, X. H.; Chen, X. F.; Chai, C. P.; Zhou, Q. F. *J. Polym. Sci., Part A: Polym. Chem.* **2006**, *44*, 4656–4667.
(55) Zhao, X. D.; Lin, W. R.; Song, N. H.; Chen, X. F.; Fan, X. H.; Zhou, Q. F. *J. Mater. Chem.* **2006**, *16*, 4619–4625.
(56) Viswanathan, G.; Chakrapani, N.; Yang, H.; Wei, B.; Chung, H.; Cho, K.; Ryu, C. Y.; Ajayan, P. M. *J. Am. Chem. Soc.* **2003**, *125*, 9258–9259.
(57) Chen, S. M.; Chen, D. Y.; Wu, G. Z. *Macromol. Rapid Commun.* **2006**, *27*, 882–887.
(58) Liu, I. C.; Huang, H. M.; Chang, C. Y.; Tsai, H. C.; Hsu, C. H.; Tsiang, R. C. C. *Macromolecules* **2004**, *37*, 283–287.
(59) Xu, Y. Y.; Gao, C.; Kong, H.; Yan, D. Y.; Jin, Y. Z.; Watts, P. C. P. *Macromolecules* **2004**, *37*, 8846–8853.
(60) Zeng, H. L.; Gao, C.; Yan, D. Y. *Adv. Funct. Mater.* **2006**, *16*, 812–818.
(61) Qu, L. W.; Veca, L. M.; Lin, Y.; Kitaygorodskiy, A.; Chen, B. L.; McCall, A. M.; Connell, J. W.; Sun, Y. P. *Macromolecules* **2005**, *38*, 10328–10331.
(62) Kong, H.; Gao, C.; Yan, D. *J. Am. Chem. Soc.* **2004**, *126*, 412–413.
(63) Yao, Z.; Braidy, N.; Botton, G. A.; Adronov, A. *J. Am. Chem. Soc.* **2003**, *125*, 16015–16024.
(64) Baskaran, D.; Mays, J. W.; Bratcher, M. S. *Angew. Chem., Int. Ed.* **2004**, *43*, 2138–2142.
(65) Takizawa, K.; Nulwala, H.; Thibault, R. J.; Lowenhielm, P.; Yoshinaga, K.; Wooley, K. L.; Hawker, C. J. *J. Polym. Sci., Part A: Polym. Chem.* **2008**, *46*, 2897–2912.
(66) Thibault, R. J.; Takizawa, K.; Lowenheilm, P.; Helms, B.; Mynar, J. L.; Frechet, J. M. J.; Hawker, C. J. *J. Am. Chem. Soc.* **2006**, *128*, 12084–12085.
(67) Joralemon, M. J.; O'Reilly, R. K.; Hawker, C. J.; Wooley, K. L. *J. Am. Chem. Soc.* **2005**, *127*, 16892–16899.
(68) Joralemon, M. J.; O'Reilly, R. K.; Matson, J. B.; Nugent, A. K.; Hawker, C. J.; Wooley, K. L. *Macromolecules* **2005**, *38*, 5436–5443.
(69) Whittaker, M. R.; Urbani, C. N.; Monteiro, M. J. *J. Am. Chem. Soc.* **2006**, *128*, 11360–11361.
(70) Shen, X.; Liu, H.; Li, Y.; Liu, S. *Macromolecules* **2008**, *41*, 2421–2425.
(71) Helms, B.; Mynar, J. L.; Hawker, C. J.; Frechet, J. M. J. *J. Am. Chem. Soc.* **2004**, *126*, 15020–15021.
(72) Killops, K. L.; Campos, L. M.; Hawker, C. J. *J. Am. Chem. Soc.* **2008**, *130*, 5062–5064.
(73) Gao, H.; Matyjaszewski, K. *J. Am. Chem. Soc.* **2007**, *129*, 6633–6639.
(74) Gao, H.; Louche, G.; Sumerlin, B. S.; Jahed, N.; Golas, P.; Matyjaszewski, K. *Macromolecules* **2005**, *38*, 8979–8982.
(75) Tsarevsky, N. V.; Sumerlin, B. S.; Matyjaszewski, K. *Macromolecules* **2005**, *38*, 3558–3561.
(76) Gao, H.; Matyjaszewski, K. *Macromolecules* **2006**, *39*, 4960–4965.
(77) Xu, J.; Ye, J.; Liu, S. *Macromolecules* **2007**, *40*, 9103–9110.
(78) Zhang, J.; Zhou, Y.; Zhu, Z.; Ge, Z.; Liu, S. *Macromolecules* **2008**, *41*, 1444–1454.
(79) Malkoch, M.; Thibault, R. J.; Drockenmuller, E.; Messerschmidt, M.; Voit, B.; Russell, T. P.; Hawker, C. J. *J. Am. Chem. Soc.* **2005**, *127*, 14942–14949.
(80) Binks, B. P.; Fletcher, P. D. I. *Langmuir* **2001**, *17*, 4708–4710.
(81) Erhardt, R.; Boker, A.; Zettl, H.; Kaya, H.; Pyckhout-Hintzen, W.; Krausch, G.; Abetz, V.; Müller, A. H. E. *Macromolecules* **2001**, *34*, 1069–1075.
(82) Xu, H.; Erhardt, R.; Abetz, V.; Müller, A. H. E.; Godel, W. A. *Langmuir* **2001**, *17*, 6787–6793.

(83) Erhardt, R.; Zhang, M.; Boker, A.; Zettl, H.; Abetz, C.; Frederik, P.; Krausch, G.; Abetz, V.; MüllerA. H. E. *J. Am. Chem. Soc.* **2003**, *125*, 3260–3267.
(84) Liu, Y. F.; Abetz, V.; Müller, A. H. E. *Macromolecules* **2003**, *36*, 7894–7898.
(85) Walther, A.; Andre, X.; Drechsler, M.; Abetz, V.; Müller, A. H. E. *J. Am. Chem. Soc.* **2007**, *129*, 6187–6198.
(86) Glaser, N.; Adams, D. J.; Boker, A.; Krausch, G. *Langmuir* **2006**, *22*, 5227–5229.
(87) Jorio, A.; Pimenta, M. A.; Filho, A. G. S.; Saito, R.; Dresselhaus, G.; Dresselhaus, M. S. *New J. Phys.* **2003**, *5*, 139.1–139.17.
(88) Fischer, D.; Potschke, P.; Brunig, H.; Janke, A. *Macromol. Symp.* **2005**, *230*, 167–172.
(89) Dresselhaus, M. S.; Dresselhaus, G.; Jorio, A.; Souza Filho, A. G.; Pimenta, M. A.; Saito, R. *Acc. Chem. Res.* **2002**, *35*, 1070–1078.
(90) Wollman, E. W.; Kang, D.; Frisbie, C. D.; Lorkovic, I. M.; Wrighton, M. S. *J. Am. Chem. Soc.* **1994**, *116*, 4395–4404.
(91) Kong, H.; Gao, C.; Yan, D. *J. Mater. Chem.* **2004**, *14*, 1401–1405.

MA801696Z